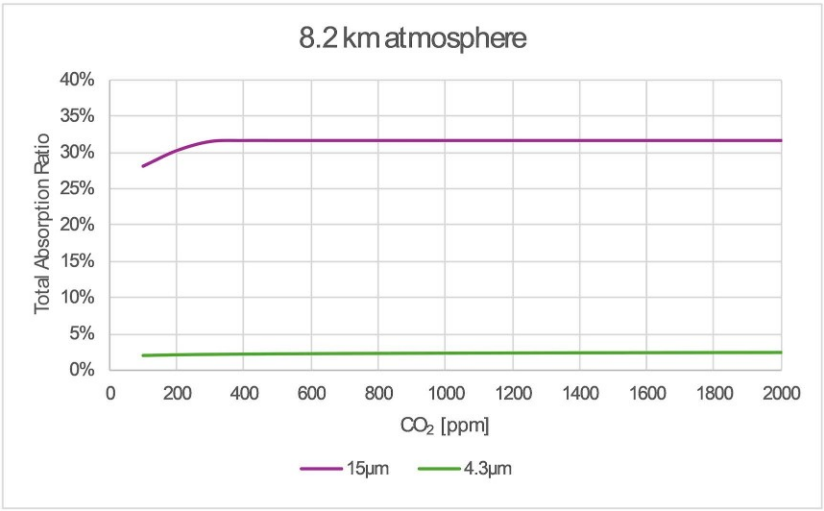

Figure 15. Absorption ratios for the two strong CO_2 absorption bands [11].

An increase from 400 to 800 ppm in CO_2 shows no measurable increase in IR absorption for the 15 μ and 4.3 μ bands and therefore total saturation. Other elaborate studies [14] estimate the total terrestrial long wavelength absorptivity a_{LW}.

$$a(L)=\frac{\int_0^\infty I_\lambda(0)\cdot a_\lambda(L)d\lambda}{\int_0^\infty I_\lambda(0)d\lambda}\times 100\% \tag{16}$$

and obtain the following results for different latitudes.

Table 2. Calculated a_{LW} from Harde [14] for various CO_2 concentrations.

CO_2 (ppm)	absorptivities ε (%)				
	tropics	mid-latitudes	high-latitudes	average 3 zones	global mean
0	81.90	69.44	58.98	74.68	77.02
35	83.80	74.48	67.04	78.43	80.08
70	84.18	75.35	68.32	79.10	80.62
140	84.65	76.31	69.80	79.86	81.29
210	84.99	77.00	70.77	80.40	81.76
280	85.28	77. 51	71.52	80.83	82.14
350	85.53	77.95	72.14	81.19	82.45
380	85.65	78.12	72.38	81.34	82.58
420	85.76	78.33	72.68	81.51	82.74
490	85.91	78.67	73.16	81.80	83.00
560	86.16	78.98	73.61	82.06	83.24
630	86.35	79.29	74.02	82.32	83.46
700	86.52	79.58	74.41	82.56	83.68
770	86.69	79.85	74.78	82.79	83.88

The next figure (**Figure 16**) shows the global mean values of the table above. While our previous model neglected the layered structure by assuming an isobar atmosphere, Harde [14] was taking the barometric effects into account.

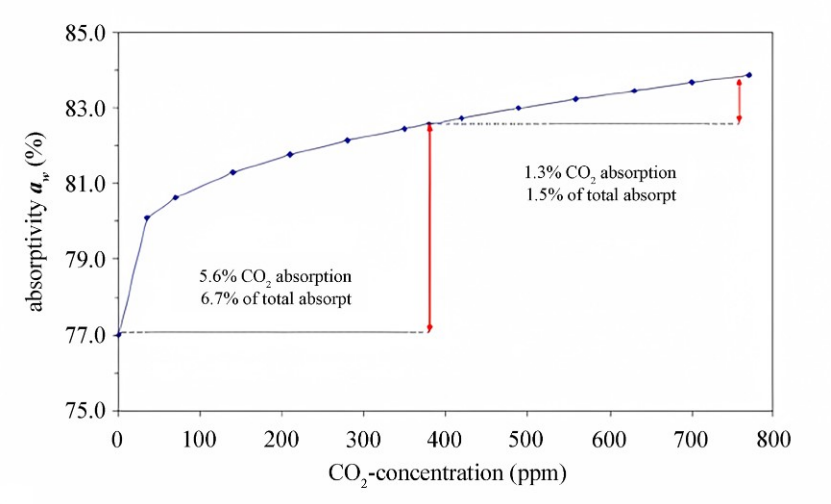

Figure 16. Influence of doubling CO_2 concentration on total absorptivity [14].

This study shows an upper limit of additional ATE by 1.5%. Average surface temperatures of $T_S = 288^{\circ}$K correspond to 390 Wm^{-2} black body radiation. From the foregoing considerations, we learned that doubling CO_2 atmospheric concentrations from 400 to 800 ppm amounts to a maximum 1.5% change of energy absorbed in the atmosphere, *i.e.* a maximal 3 Wm^{-2} of back-radiation increase. Using the Stefan-Boltzmann formula we then obtain a first estimation of a corresponding temperature increase or GH contribution of 0.5˚K by having 800 ppm atmospheric content compared to the current 400 ppm. This also corresponds very well with the results from Wijngaarden and Happer [2].

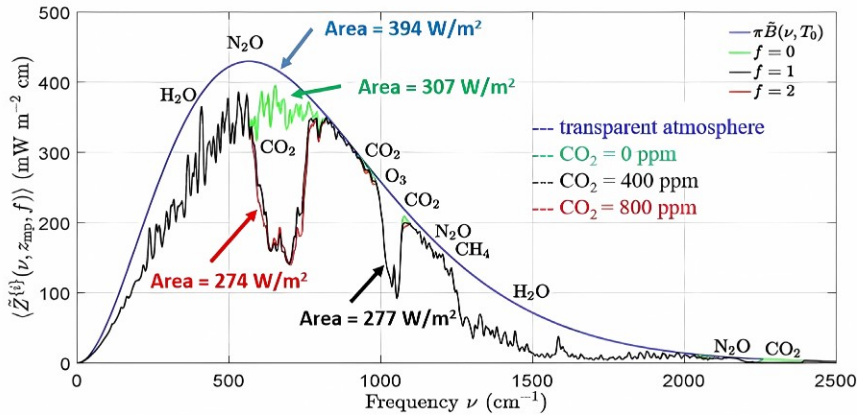

Figure 17. Total atmospheric absorptivity changes by CO_2 increases calculated by Wijngaarden and Happer [2].

Ground measurements fall in line with **Figure 17** and indicate almost complete

saturation of IR absorption in our atmosphere. We were therefore interested in designing a simple and independent low-cost experimental setup to demonstrate this saturated behavior. This setup and the results obtained will be described in the following section.

2. Experimental Methods

The aim of this work was therefore to demonstrate in a simple manner that an IR-active gas can indeed influence the heat radiation of a body. Another aim was to demonstrate that CO_2 back-radiation is limited by saturation of absorbance. This was realized by two different experimental setups.

The measurements should allow us to learn if the saturation behavior measured by others and discussed in the foregoing sections of this work are indeed correct and draw conclusions towards the question of CO_2-induced global warming.

According to the second law of thermodynamics, heat flows from hotter to colder objects ("downhill"), unless energy in some form is supplied to reverse the direction of heat flow or there is a medium that absorbs part of the energy and remits it isotropic, like greenhouse models describe the radiation household within our atmosphere. Our test atmospheres were studied against a −25˚C cooled black disc ("Lab Mode") or a cloudless night sky ("Outdoor or Field Mode") using the natural IR source of surface and atmospheric back radiation.

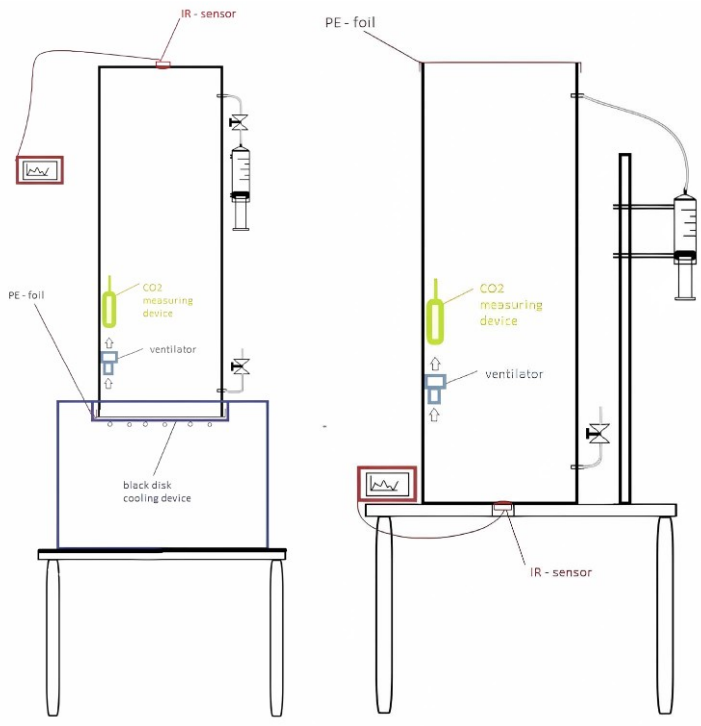

(a) (b)

Figure 18. experimental setup for (a) "Lab Mode" using a cooling compressor and (b) "Field Mode".

Translating these setups into energy flow diagrams like in Figure 3 & Figure 4 we first analyze Figure 18(a).

As shown in Figure 19 the "Lab Mode" IR sensor response is solely determined by the back-radiation from Test Atmosphere 2 with increasing CO_2 concentrations. The cold plate on the other side of the test cylinder allows thermal flow according to the second law of thermodynamics. Inside the volume of the test cylinder, a CO_2 detector and a low-power ventilator are mounted and run by a combined power pack. The communication with the CO_2 detector is performed via Bluetooth. β is the intensity ratio $\beta = A_D \sin^2\theta$ for an IR detector with numerical aperture θ within the cylindrical test column and the detector area A_D of 1 cm². ε_2 solely depends on the GH gas concentrations in the test tube and the intensity $\frac{\beta}{2}\varepsilon_1\varepsilon_2\sigma T_1^4$ is measured by a Thermopile IR detector from Thorlabs®.

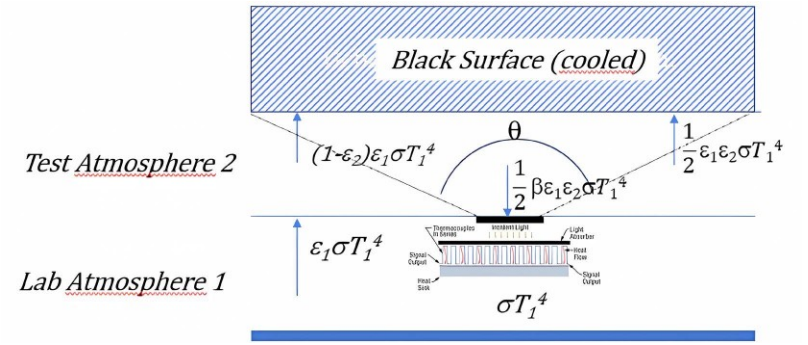

Figure 19. "Lab Mode" test bench with cooled black disc.

In the "Field Mode (Figure 18(b)) the test cylinder is rotated by 180˚, the cooling compressor is removed and replaced by the clear night sky. The temperature gradient in this case is the difference between T_S and T_E, where T_E is derived from (7)

$$T_E = 4\sqrt{\frac{\left(1+KC^2\right)\cdot 8.78\cdot 10^{-13}\cdot T_S^{5.852}\cdot RH^{0.07195}}{\sigma}} \tag{17}$$

The down-dwelling radiation through the test chamber into the IR detector is determined by

$$P = \beta e_1 e_2 s T_E^4 \tag{18}$$

Using the parametrization of Howard [11] we obtain for CO_2 test atmospheres power densities below the detection limit of the IR sensor of 10 μW/cm² in this setup. Using stronger GH gases would significantly increase ε_1 as we have tested in our experimental series. This would prove that CO_2 is a relatively weak greenhouse gas even when increasing its concentration into the percentage region, compared to other GH gases, which would be detectable already at relatively low concentrations.

3. Results

The 7-liter test cylinder in Figure 18(a) was filled up with pure nitrogen. CO_2 was

added in 50 ml steps. Simultaneously the CO_2 detector was used to measure the concentration while the ventilator was trying to homogenize the gas volume admixture. In Figure 20 the obtained power values of the IR detector are plotted.

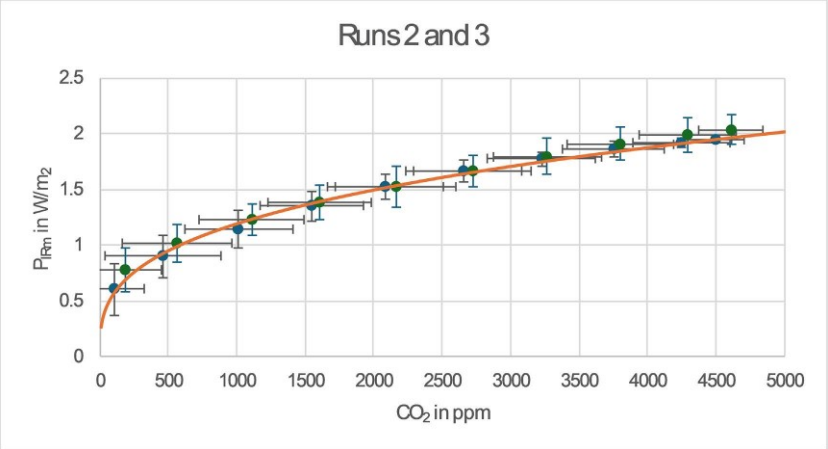

Figure 20. Run 2.2 and Run 2.3 in the Lab Mode mixing CO_2 into a pure nitrogen atmosphere.

From previous considerations, we can estimate the back-radiation by the parametrization of Howard [11] (Equations (14)-(15)).

Low values of absorption length are outside the fit and measurement range of Howard but serve as extrapolations to estimate orders of magnitude. The trend in Figure 21 is indeed very similar to the measured values in Figure 20 and confirms the logarithmic behavior of the absorption.

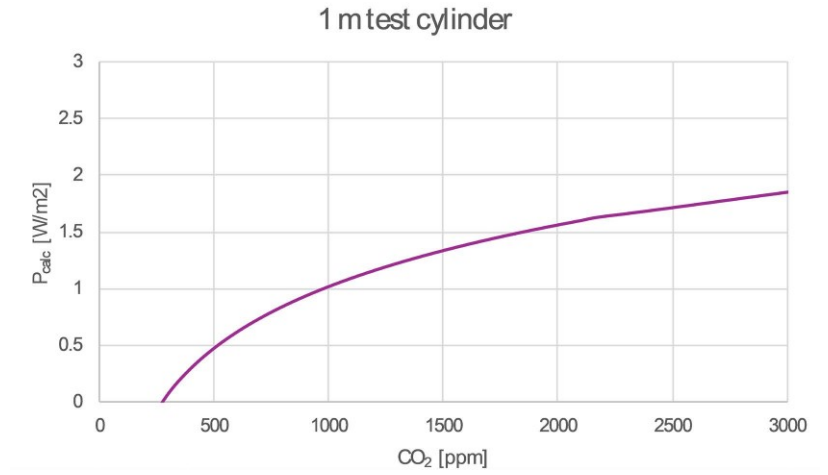

Figure 21. P calculated from Howard [11].

Using the values plotted in Figure 20 we can estimate the fractional absorbance A_f for varying CO_2 concentrations in N_2 atmospheres

$$\ln\left(\frac{I_0}{I_1}\right) = \varepsilon \cdot c \cdot d \tag{19}$$

where c is the molar concentration (mol·m^{-3}) and d air column length (m). We use the Beer-Lambert law (13) function, where ε. is the absorption coefficient of our test atmosphere to obtain

$$A_f = \frac{I_o - I}{I} = \left(1 - e^{-\varepsilon \cdot c.d}\right) \tag{20}$$

Using (20) it is possible to calculate the back-radiation for a given air column length (Figure 22) at ground-level conditions for saturation at a given ppm CO_2.

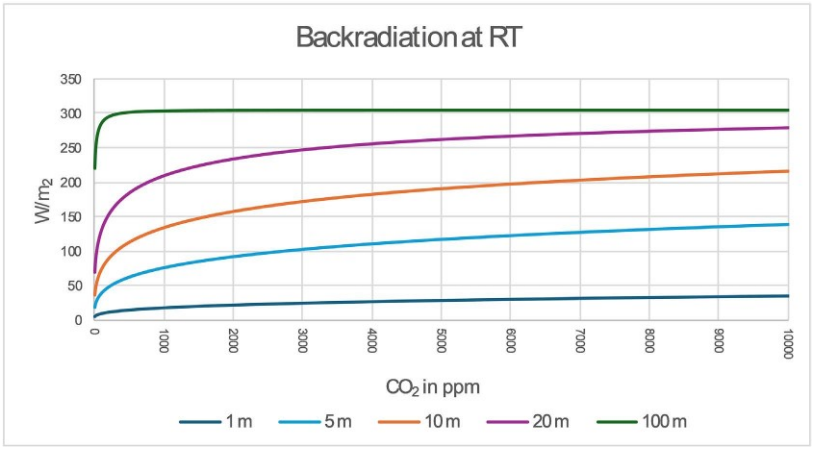

Figure 22. Calculated back-radiation for different long air columns at room temperature (RT).

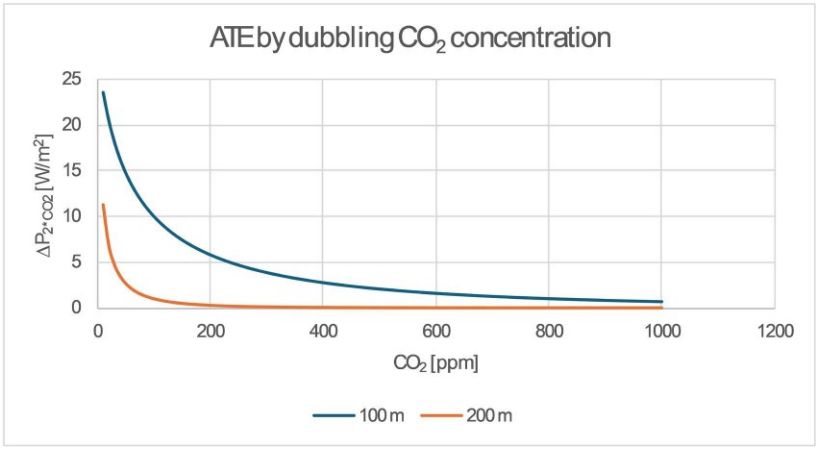

Figure 23. Calculated effect of CO_2 doubling on backscattered power in two air columns.

In Figure 23 we calculated the corresponding atmospheric thermal enhancement (ATE) when doubling the actual CO_2 concentration for a homogeneous atmosphere of 100 m thickness at 1 bar. The result shows a rapid reduction in ATE with increasing the length of the air columns. Applying this result to the real world means saturation in CO_2 concentration with respect to measurable thermal effects. This will be discussed in more detail in the next chapter.

Figure 24 was the result obtained in the so-called Field Measurements against a black cloudless night sky. There is a clear indication that no measurable

backscattering is observable when adding CO_2 from 0 to 5000 ppm to the system. Equation (9) with ε_1-0.2, $\varepsilon_2 < 0.2$ and β-0.02 gives $\beta\varepsilon_1\varepsilon_2 < 0.0004$ and therefore $P = \beta\varepsilon_1\varepsilon_2\sigma T_E^4 < 3 \times 10^{-2}$ W/m^2 = 3 μW/cm^2. The working power of the used Thermopile Thorlabs detector with 1 cm^2 active area starts at 10 μW. For stronger GH gases it would be possible to exceed the detection limits and obtain a response. This was shown by using the Freon gas $C_2H_2F_4$ as shown in the next figure.

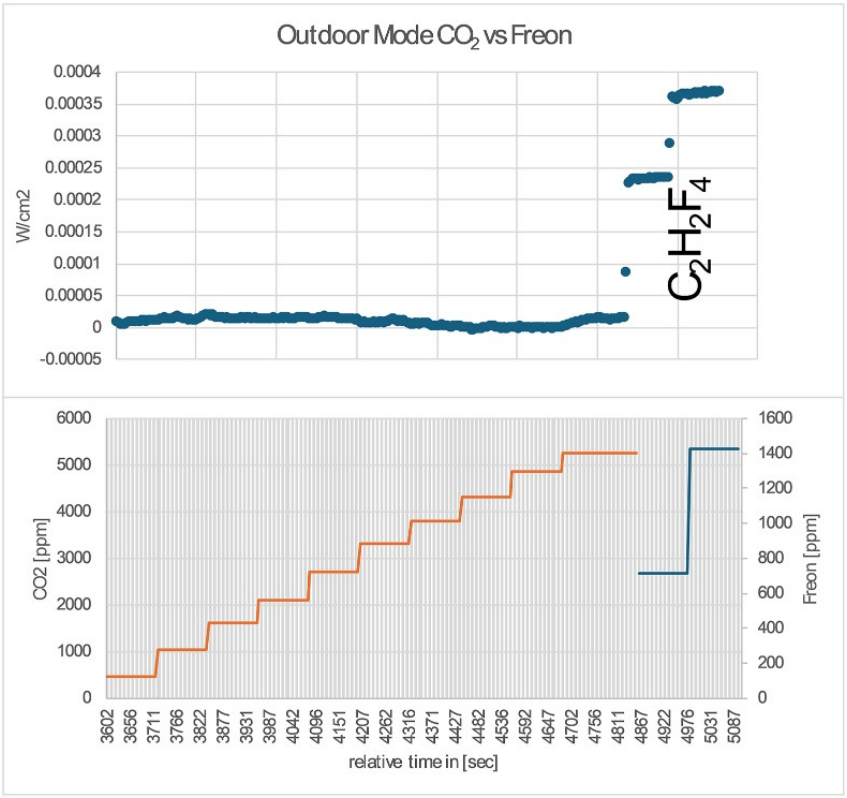

Figure 24. Field Mode comparative measurement CO_2 and Freon ($C_2H_2F_4$).

The detector was indeed reacting when $C_2H_2F_4$ Freon was added up to 1400 ppm. The measured absorbance of $C_2H_2F_4$ by NIST [15] (**Figure 25**) is indeed, up to 100 times stronger than CO_2 measured by the same institution [16] (**Figure 26**).

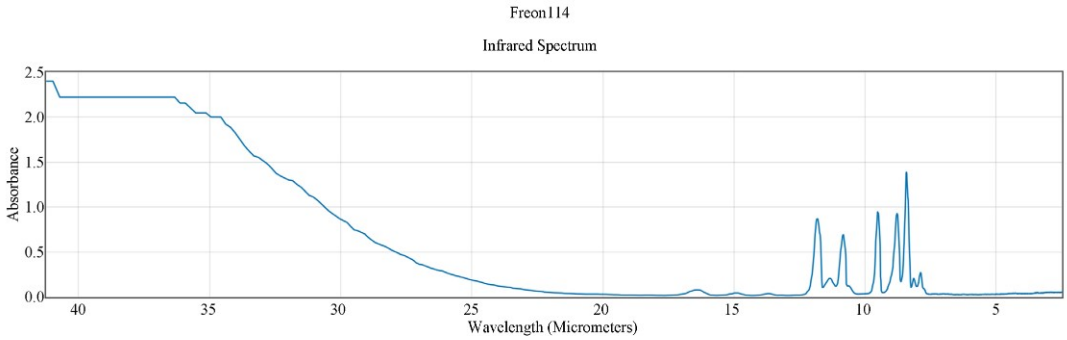

Figure 25. Absorbance of Freon ($C_2H_2F_4$) [15].

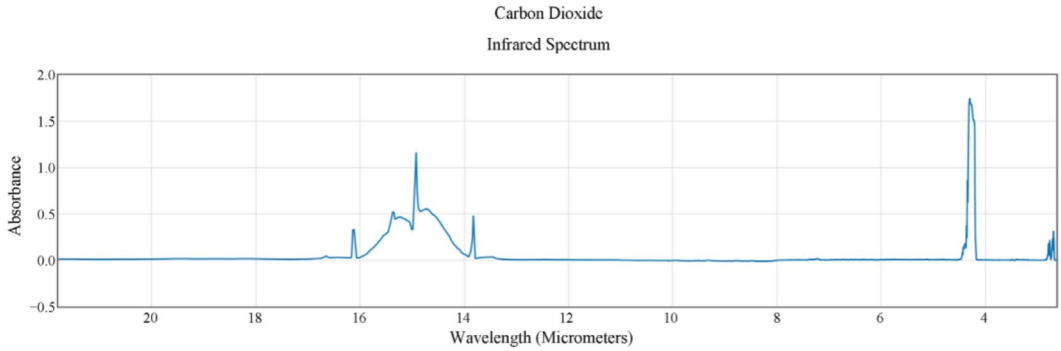

Figure 26. Absorbance of carbon dioxide (CO_2) [16].

4. Discussion

Atmospheric windows, especially the optical and infrared, affect the distribution of energy flows and temperatures within Earth's energy balance. The windows depend upon clouds, water vapor, trace greenhouse gases, and other components of the atmosphere.

Out of an average of 341 watts per square meter (W/m^2) of solar irradiance at the top of the atmosphere, about 161 W/m^2 reaches the surface via atmospheric windows and through clouds (albedo). IR absorption by the atmosphere and corresponding atmospheric heating leads to an equilibrium of 333 W/m^2 of back-radiation and outgoing LW surface radiation of 396 W/m^2 latent heat from evaporation (80 W/m^2) and other thermal losses (17 W/m^2). Our measurements align with limitations to an increase of maximum 3W/m^2 back-radiation by doubling the CO_2 content from 400 to 800 ppm. This minor contribution should not exceed a temperature increase of more than 0.5˚K a value, which is not within the range of significant impact for climatic changes and much lower than annual temperature variations in all regions of the earth.

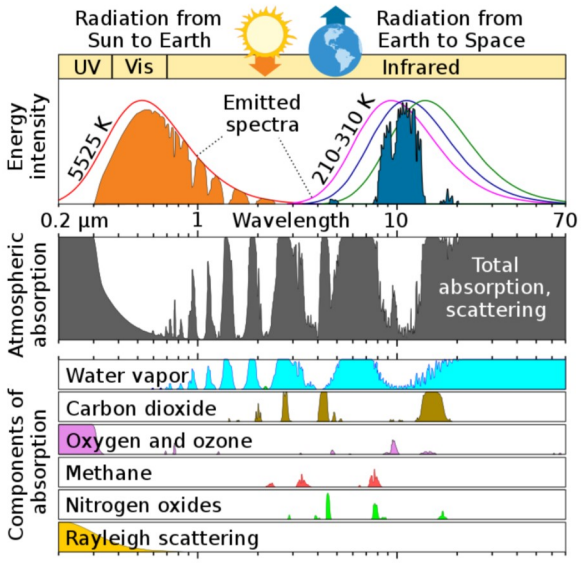

Figure 27. "The Atmospheric Window", NOAA [17] [18].

From **Figure 27** it should be obvious that only minor contributions can be obtained from the edges of the two prominent CO_2 windows. Water vapor is indeed the major absorber and other GH gases are not relevant at their current concentrations. Increased water vapor should also lead to cloud coverage at constant aerosol concentrations. Slight variations of solar constants and cosmic rays using balanced feedback loops should allow for long-term thermal equilibrium. Fluctuations are often due to unnatural time scales, long-time constants, and statistical noise. In a simplified picture, where we consider an atmosphere with uniform density corresponding to the surface density $\rho = 1.2225\ \mathrm{kg{\cdot}m^{-3}}$ we obtain an atmospheric air column weight of 10,300 $\mathrm{kg{\cdot}m^{-2}}$ at a length of 8425 m. From our measurements and a simple Beer-Lambert model of such an air column, we found (**Figure 13**) already at 200 m complete saturation at current CO_2 concentrations, without significant contributions to further ATE. Schildknecht [19] using similar arguments finds that doubling of the CO_2 content in air from 380 ppm to 760 ppm in one century is an increase of $\Delta T \simeq 0.5^{\circ}C$, which corresponds well with the expected values of this and other works.

Our results should therefore contribute to previously accepted findings which do not indicate any reason to cause climate run-aways by increased CO_2 contents. Ekholm [20] introduced the idea of fictitious atmospheric radiation levels due to CO_2 increase. According to him secular cooling of the earth is the principal cause of variation in the quantity of carbon dioxide in the atmosphere. He explained how carbon dioxide is a key player in the greenhouse effect and how his conclusion was based on the earlier work of Fourier, Pouillet, Tyndall, and others. According to their estimations, a tripling of carbon dioxide levels will raise global temperatures by 7˚C to 9˚C. An increase in carbon dioxide should heat high latitudes more than the tropics and create a warmer more uniform climate over the entire Earth. Hansen [21] testified this before Congress and raised public awareness of climate change. Hansen was claiming "The most powerful feedback is provided by water vapor". While this argument seems strong it must be questioned considering paleoclimatic facts e.g. higher temperatures in the Eemian interglacial period 120,000 years ago and the Holstein interglacial period 5,000 to 15,000 years ago did not trigger a tipping point or a galloping greenhouse effect. Sarker [22] mentions correctly that 0.24 gigatons of carbon were emitted into the atmosphere for 50,000 years to cause this severe warming known as the *PETM*. In comparison, humans emit 10 gigatons, or approximately fifty times that amount of carbon annually, into the atmosphere. There is no doubt that a warming climate has negative impacts on various important properties, such as the aridity index for rivers [23]. Even just studying rivers there are many other anthropogenic impacts not related to CO_2 which dramatically influence their current and future environmental integrity [24] [25]. Current global warming can be natural and/or anthropogenic. To be sure, we must understand how it was possible to obtain 100 m higher sea levels or to end up by glaciation over large areas of landmasses without anthropogenic CO_2 emission triggers. Additional energy or energy loss was due to

natural forces which must be fully understood before drawing wrong conclusions. Ice core data do not indicate fundamental different temperature variations over the last 10,000 years. We also need a better understanding of the validity of power flow diagrams as published by the IPCC. It would be a great success of our efforts if such questions could be reconsidered also considering the results presented in this work.

5. Conclusion

Experimental evidence in this work confirms earlier work that increasing levels of CO_2 at current levels in the atmosphere cannot significantly contribute to warming by more back-radiation. We also demonstrated that increasing greenhouse spurious gases like Freon show a strong response in back-radiation when added into our atmospheric test chamber. Climate models and their CO_2 forcings should be revised and much more experimental evidence about the IR radiation response of greenhouse gases should be collected before appointing current warming trends and climate change mechanisms monocausal to greenhouse gas theories.

Conflicts of Interest

The authors declare no conflicts of interest regarding the publication of this paper.

References

[1] European Parliament (2023) Fortschritte der EU bei der Verwirklichung ihrer Klimaziele für 2020 (Infografik). https://www.europarl.europa.eu/news/de/headlines/society/20180706STO07407/fortschritte-der-eu-bei-der-verwirklichung-ihrer-klimaziele-infografik?at_campaign=20234-Green&at_medium=Google_Ads&at_platform=Search&at_creation=DSA&at_goal=TR_G&at_audience=&at_t

[2] van Wijngaarden, W.A. and Happer, W. (2020) Dependence of Earth's Thermal Radiation on Five Most Abundant Greenhouse Gases. arXiv: 2006.03098. https://doi.org/10.48550/arXiv.2006.03098

[3] Happer, W. and Lindzen, R. (2022) Comment and Declaration on the SEC's Proposed Rule "The Enhancement and Standardization of Climate-Related Disclosures for Investors," File No. S7-10-22, 87 Fed. Reg. 21334. https://www.sec.gov/comments/s7-10-22/s71022-20132171-302668.pdf

[4] Barrett, J. (2005) Greenhouse Molecules, Their Spectra and Function in the Atmosphere. *Energy & Environment*, **16**, 1037-1045. https://doi.org/10.1260/095830505775221542

[5] James, I.N. (1994). Introduction to Circulating Atmospheres. Cambridge University Press. https://doi.org/10.1017/cbo9780511622977

[6] https://web.archive.org/web/20230329191117/www.acs.org/climatescience/atmosphericwarming/multilayermodel.html

[7] Swinbank, W.C. (1963) Long-Wave Radiation from Clear Skies. *Quarterly Journal of the Royal Meteorological Society*, **89**, 339-348. https://doi.org/10.1002/qj.49708938105

[8] Goforth, M.A., Gilchrist, G.W. and Sirianni, J.D. (2002) Cloud Effects on Thermal Downwelling Sky Radiance. *Proceedings of SPIE-The International Society for*

Optical Engineering 4710, Orlando, 15 March 2002. https://doi.org/10.1117/12.459570

[9] Petty, G.W. (2006) A First Course in Atmospheric Radiation. Sundog Publishing, 223.

[10] Angström, A. (1918) Smithsonian Inst., Misc. Coll., 65, 3. https://www.realclimate.org/images/Angstrom.pdf

[11] Howard, J.N., Burch, D.E. and Williams, D. (1956) Infrared Transmission of Synthetic Atmospheres II Absorption by Carbon Dioxide. *Journal of the Optical Society of America*, **46**, 237-241. https://doi.org/10.1364/josa.46.000237

[12] Fröhlich, C., Philipona, R. and Marty, C. (1998,) Untersuchung des Oberflächenstrahlungshaushaltes in den Alpen und im Vergleich zum schweizerischen Mittelland. VDF Hochschulverlag AG an der ETH Zürich.

[13] Makhdoumi Akram, M., Nikfarjam, A., Hajghassem, H., Ramezannezhad, M. and Iraj, M. (2020) Low Cost and Miniaturized NDIR System for CO_2 Detection Applications. *Sensor Review*, **40**, 637-646. https://doi.org/10.1108/sr-06-2019-0140

[14] Harde, H. (2014) Advanced Two-Layer Climatemodel for the Assessment of Global Warming by CO_2. *Open Journal of Atmospheric and Climate Change*, **1**, 1-51.

[15] $C_2Cl_2F_4$. https://webbook.nist.gov/cgi/cbook.cgi?ID=C76142&Type=IR-SPEC&Index=2

[16] CO_2. https://webbook.nist.gov/cgi/cbook.cgi?ID=C124389&Units=SI&Type=IR-SPEC&Index=1#IR-SPEC

[17] National Oceanic and Atmospheric Administration (2023) The Atmospheric Window. https://www.noaa.gov/jetstream/satellites/absorb

[18] US Department of Commerce, NOAA. The Earth-Atmosphere Energy Balance. https://www.weather.gov/

[19] Schildknecht, D. (2020) Saturation of the Infrared Absorption by Carbon Dioxide in the Atmosphere. *International Journal of Modern Physics B*, **34**, Article 2050293. https://doi.org/10.1142/s0217979220502938

[20] Ekholm, N. (1901) On the Variations of the Climate of the Geological and Historical Past and Their Causes. *Quarterly Journal of the Royal Meteorological Society*, **27**, 1-62. https://doi.org/10.1002/qj.49702711702

[21] Hansen, J., Johnson, D., Lacis, A., Lebedeff, S., Lee, P., Rind, D., *et al.* (1981) Climate Impact of Increasing Atmospheric Carbon Dioxide. *Science*, **213**, 957-966. https://doi.org/10.1126/science.213.4511.957

[22] Sarker, S. (2022) Fundamentals of Climatology for Engineers: Lecture Note. *Eng*, **3**, 573-595. https://doi.org/10.3390/eng3040040

[23] Sarker, S. (2021) Investigating Topologic and Geometric Properties of Synthetic and Natural River Networks under Changing Climate. https://stars.library.ucf.edu/etd2020/965

[24] Gao, Y., Sarker, S., Sarker, T. and Leta, O.T. (2022) Analyzing the Critical Locations in Response of Constructed and Planned Dams on the Mekong River Basin for Environmental Integrity. *Environmental Research Communications*, **4**, Article 101001. https://doi.org/10.1088/2515-7620/ac9459

[25] Sarker, S., Veremyev, A., Boginski, V. and Singh, A. (2019) Critical Nodes in River Networks. *Scientific Reports*, **9**, Article No. 11178. https://doi.org/10.1038/s41598-019-47292-4